Inorg. Chem. **1993**, *32*, 3689-3693

Synthesis, Structure, and Emission Spectroscopy of Luminescent Pt(COD)(dithiolate) Complexes

Joanne M. Bevilacqua, Juan A. Zuleta, and Richard Eisenberg*

Department of Chemistry, University of Rochester, Rochester, New York 14627

Received November 25, 1992

The synthesis, characterization, X-ray structure determination and emission spectroscopy of two Pt(COD)(S-S) complexes are reported where COD = 1,5-cyclooctadiene (COD) and S-S is maleonitriledithiolate (mnt) for complex **1** and 1-(ethoxycarbonyl)-1-cyanoethylene-2,2-dithiolate (ecda) for complex **2**. Both complexes are isolated in high yield from the reaction of $Pt(COD)Cl_2$ and the corresponding dianionic dithiolate salt. Orange crystals of **1** ($C_{12}H_{12}N_2PtS_2$) are monoclinic, space group $P2_1/n$ (No. 14), with $a = 9.539(9)$ Å, $b = 8.944(4)$ Å, $c = 15.145(6)$ Å, $\beta = 100.69(7)°$, $V = 1269.66$ Å^3, $Z = 4$, and final $R = 0.0257$ ($R_w = 0.0346$) for 2391 unique reflections. Yellow crystals of **2** ($C_{14}H_{17}NO_2PtS_2$) are triclinic, space group $P\bar{1}$ (No. 2), with $a = 7.561(5)$ Å, $b = 9.787(8)$ Å, $c = 11.747(6)$ Å, $\alpha = 66.42(8)°$, $\beta = 77.30(0)°$, $\gamma = 83.71(5)°$, $V = 776.97$ Å^3, $Z = 2$, and final $R = 0.0385$ ($R_w = 0.0489$) for 2430 unique reflections. Each complex possess a square planar structure with chelating diolefin and dithiolate ligands. Proton NMR spectroscopy shows that the solid-state structures are maintained in solution. The complexes are luminescent at low temperature in the solid state and in frozen glasses. In the solid state at 77 K, Pt(COD)(mnt) exhibits a highly structured emission ($\lambda_{max} = 560$ nm, 17.9 kcm^{-1}) with a vibronic progression of ~1400 cm^{-1}, whereas for Pt(COD)(ecda), the emission is broad and featureless ($\lambda_{max} = 525$ nm, 19.0 kcm^{-1}). The emissive state for both complexes is assigned as a metal-to-dithiolate charge transfer with differences in the structure and energy of the emissions resulting from differences in the $\pi^*_{dithiolate}$ orbital of the mnt and ecda ligands.

Introduction

During the last 5 years, complexes of Pt(II) containing dithiolate and diimine ligands have been the focus of considerable study in our laboratory because of their solvatochromic behavior and room temperature luminescence in fluid solution.[1-4] Particular attention has been paid to the influence of ligands on the optical properties of these systems, especially with regard to the dianionic ligand as either the 1,2-dithiolate maleonitriledithiolate (mnt) or the 1,1-dithiolate 1-(ethoxycarbonyl)-1-cyanoethylene-2,2-dithiolate (ecda). It was observed that while the absorption spectra of Pt(diimine)(dithiolate) complexes for a given diimine (bipyridine, *o*-phenanthroline, or alkylated derivatives) exhibited similar solvatochromic behavior, the emission spectra showed strikingly different band shapes. Specifically, emission bands from mnt complexes were highly structured, while ecda analogues possessed essentially featureless emissions. Moreover, from lifetime measurements as a function of temperature, the mnt complexes were observed to have single exponential behavior, while the ecda complexes gave evidence of multiple emitting states. On the basis of these results and on molecular orbital calculations, different emitting states were assigned to the platinum(II) diimine complexes of mnt and ecda, with the mnt systems having a (Pt(d)/S(p)–$\pi^*_{dithiolate}$) emissive state and the ecda complexes possessing a (Pt(d)/S(p)–$\pi^*_{diimine}$) lowest energy emission. The difference in the emitting states was thought to arise from the difference in the $\pi^*_{dithiolate}$ energies for mnt and ecda relative to the lowest unoccupied π^* level of the diimine.

To probe further the electronic structural differences between mnt and ecda coordinated to Pt(II) in PtL_2(S-S) systems, the corresponding complexes with L_2 = 1,5-cyclooctadiene (COD) have been synthesized and characterized fully. The mnt complex Pt(COD)(mnt) (**1**) had previously been reported and partially characterized by Johnson *et al.*[5] The present study describes the synthesis and characterization of the ecda complex **2** as well as

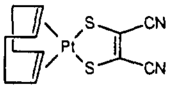

1

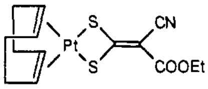

2

the single-crystal X-ray structure determination of both systems. In accord with the absence of a low-lying $\pi^*_{diimine}$ level, neither complex exhibits the solvatochromic behavior or the room-temperature fluid solution emission of the diimine dithiolate complexes. However, both complexes are luminescent at 77 K, and, as with the diimine analogues, they show significant differences in their emission spectra.

Experimental Section

Materials, Methods, and Preparations. The reagent K_2PtCl_4 (Johnson Matthey) was used as received without further purification. The compounds Pt(COD)(mnt) (**1**),[5] Na_2(mnt),[6] K_2(ecda),[7] and $Pt(COD)Cl_2$[8] were prepared according to literature methods. Syntheses were performed under N_2 using standard Schlenk and inert atmosphere techniques. All solvents were of spectral grade quality and were dried, distilled, and rigorously degassed before use.

Pt(COD)(ecda) (2). A degassed solution of 0.80 g (3.13 mmol) of K_2(ecda) in 20 mL of methanol was added to 0.94 g (2.5 mmol) of $Pt(COD)Cl_2$ dispersed in 30 mL of degassed acetone and heated to ~30 °C. An intense orange solution readily formed and then faded over 3–5 min to a bright yellow solution. Upon reduction of solvent volume to ~15 mL, a yellow precipitate formed. The reaction was continued for 30 min to ensure complete precipitation. The precipitate was collected by filtration, washed first with water and then with ethanol to remove any unreacted dithiolate, and then dried with ether. The product was stored under vacuum. The IR spectrum (KBr, cm^{-1}) shows peaks due to coordinated COD by comparison with $Pt(COD)Cl_2$ and peaks assignable

---

(1) Zuleta, J. A.; Chesta, C. A.; Eisenberg, R. *J. Am. Chem. Soc.* **1989**, *111*, 8916.

(2) Zuleta, J. A.; Burberry, M. S.; Eisenberg, R. *Coord. Chem. Rev.* **1990**, *97*, 47.

(3) Zuleta, J. A.; Bevilacqua, J. M.; Eisenberg, R. *Coord. Chem. Rev.* **1991**, *111*, 237.

(4) Zuleta, J. A.; Bevilacqua, J. M.; Rehm, J. M.; Eisenberg, R. *Inorg. Chem.* **1992**, *31*, 1332.

(5) Johnson, C. E.; Eisenberg, R.; Evans, T. R.; Burberry, M. S. *J. Am. Chem. Soc.* **1983**, *105*, 1795.

(6) Davidson, A.; Holm, R. H. *Inorg. Synth.* **1967**, *10*, 8.

(7) Jensen, K. A.; Henriksen, L. *Acta Chem. Scand.* **1968**, *22*, 1108.

(8) McDermott, J. X.; White, J. F.; Whitesides, G. M. *J. Am. Chem. Soc.* **1976**, *98*, 6521.

0020-1669/93/1332-3689$04.00/0

Table I. Crystallographic Data for Pt(COD)(S-S)

	Pt(COD)(mnt) (**1**)	Pt(COD)(ecda) (**2**)
chem formula	$C_{12}H_{12}N_2PtS_2$	$C_{14}H_{17}NO_2PtS_2$
fw	443.45	490.50
lattice type	monoclinic	triclinic
space group	$P2_1/n$ (No. 14)	$P\bar{1}$ (No. 2)
Z	4	2
a, Å	9.539(9)	7.561(5)
b, Å	8.944(4)	9.787(8)
c, Å	15.145(6)	11.747(6)
α, deg	90	66.42(8)
β, deg	100.69(7)	77.30(0)
γ, deg	90	83.71(5)
V, Å^3	1269.66	776.97
ρ_{calc}, g/cm^3	2.319	2.096
T, °C	25	25
μ, cm^{-1}	114.6	93.8
$\lambda_{Mo\ K\alpha}$ (graphite monochromated radiation), Å	0.710 69	0.719 69
R	0.026	0.038
R_w	0.035	0.049

[a] $R = \{\sum\|F_o| - |F_c\|\}/\{\sum|F_o|\}$; $R_w = [\sum w(|F_o| - |F_c|)^2]^{1/2}/\{\sum wF_o^2\}$, where $w = [\sigma^2(F_o) + (\rho F_o^2)^2]^{1/2}$ for the non-Poisson contribution weighting scheme. The quantity minimized was $\sum w(|F_o|-|F_c|)^2$. Source of scattering factors f_o, f', f'': Cromer, D. T.; Waber, J. T. *International Tables for X-Ray Crystallography*; Kynoch Press: Birmingham, England, 1974; Vol. IV, Tables 2.2B and 2.3.1.

to ecda: 2207 (s, C≡N), 1697 (s, C=O), 1473 (s, C=C), 1144 (m, C—S). ^{1}H NMR ($CDCl_3$): δ 5.41 (d with Pt satellites, 4 H, $^2J_{H-H} = 23$ Hz, $^2J_{Pt-H} = 28$ Hz, vinyl H), 4.25 (q, 2 H), 2.70 (m, 4 H), 2.35 (m, 4 H), 1.35 (t, 3 H). Anal. Calcd for $C_{14}H_{17}NO_2PtS_2$: C, 34.28; H, 3.49; N, 2.85. Found: C, 33.93; H, 3.43; N, 2.71.

Physical Measurements. Infrared spectra were obtained from KBr pellets using a Mattson Sirius 100 FTIR spectrometer. ^{1}H NMR spectra (400 MHz) were recorded on a Bruker AMX-400 spectrometer. Chemical shifts are reported in ppm from an internal solvent peak (chloroform, $\delta_H = 7.24$). UV–visible spectra were recorded on a Hewlett Packard HP-8452A diode-array spectrometer in a 1-cm quartz cell at room temperature. Low temperature emission measurements were performed on deoxygenated DMM glasses (DMF/methylene chloride/methanol in 1:1:1 v/v/v) using a Spex Fluorolog fluorescence spectrophotometer fitted with a liquid nitrogen dewar equipped with quartz windows.

Low temperature lifetimes were measured by exciting the sample with a PRA Nitromite N_2 laser pumping on stilbene 420. The signal was filtered through a Corning 3-73 glass cutoff filter and American ISA monochromator with 0.5-μm slits, detected with an RCA 931C photomultiplier tube at 1200 V, and analyzed with a Tektronix 7912Ad programmable digitizer with 7A16p or 7A22 amplifier vertical plug and 71390p horizontal plug. Data analyses were performed on an IBM 9000 series computer. A least-squares routine was used to fit the lifetimes.[2]

Cyclic voltammetric experiments were carried out on a Princeton Applied Research 173 potentiostat and a PAR 175 sweep generator and a Houston 2000 XY recorder. A single-compartment, three-electrode cell containing a glassy-carbon (3.2 mm diameter) working electrode, a platinum wire auxiliary electrode, and a silver wire reference electrode were used for all measurements. Samples were dissolved in nitrogen-degassed methylene chloride with 0.11 M (TBA)PF_6 as supporting electrolyte and all potentials are referenced to ferrocene ($E_{1/2}(+/0) = 0.48$ V). The reductions are irreversible so E_p (peak potentials) are reported at scan rates of 200 mV/s.

Structure Determinations. The single-crystal X-ray structure determinations were carried out using an Enraf-Nonius CAD4 diffractometer with Mo Kα radiation ($\lambda = 0.710\ 73$ Å) for data collection. For both structure determinations, a Texsan software package was used for data reduction, structure solution, and least-squares refinement.

Crystal Structure Determination of Pt(COD)(mnt) (1). An orange prismatic crystal of Pt(COD)(mnt) (**1**), having the approximate dimensions 0.37 × 0.63 × 0.21 mm^3, was grown from a room-temperature chloroform solution. Crystal data and data collection parameters are summarized in Table I. Heavy-atom methods were employed to locate the platinum and two sulfur atoms, and subsequent cycles of least-squares refinements and difference Fourier maps located the remaining non-hydrogen atoms. Hydrogen atoms were placed at calculated positions around the cyclooctadiene ligand.

Crystal Structure Determination of Pt(COD)(ecda) (2). A crystal suitable for X-ray diffraction was grown by slow evaporation of a solution of the complex in CH_2Cl_2:CCl_4 (1:1 v/v). The crystals were found to be air stable at room temperature. An orange plate of crystal dimensions 0.40 × 0.41 × 0.15 mm^3 was mounted on a glass fiber. Crystal, data collection, and refinement parameters are summarized in Table I. Heavy-atom methods were employed to locate the platinum and two sulfur atoms. The remaining atoms were located using cycles of Fourier maps and least square refinements. In the last refinement all non-hydrogen atoms were described with anisotropic thermal parameters. Hydrogen atoms were placed at calculated positions around the cyclooctadiene ligand and the ethyl group of the dithiolate ligand.

Results and Discussion

Complexes **1** and **2** are prepared easily by reaction of Pt(COD)Cl_2 with the alkali metal salt of the corresponding dithiolate. The complexes have been characterized by FTIR spectroscopy, ^{1}H NMR spectroscopy, microanalysis, and single-crystal X-ray diffraction. The infrared spectrum of Pt(COD)(mnt) (**1**) exhibits a strong band at 2210 cm^{-1} corresponding to ν_{CN} and a single ν_{CS} stretch at 1159 cm^{-1}. The ^{1}H NMR spectrum of **1** in chloroform solution shows a singlet with Pt satellites at δ 5.63 ppm (4 H, $J_{Pt-H} = 35$ Hz) corresponding to the vinylic protons on the cyclooctadiene ligand and unresolved multiplet resonances at δ 2.8–2.5 ppm (8 H) assignable to the methylene protons of the chelating COD ligand.

Similarly, the infrared spectrum of Pt(COD)(ecda) (**2**) exhibits a strong ν_{CN} band at 2205 cm^{-1} and a single ν_{CS} signal at 1146 cm^{-1}. There is also a strong band at 1697 cm^{-1} corresponding to ν_{CO} of the ecda ligand. The ^{1}H NMR spectrum of **2** is more complicated regarding the COD resonances due to the asymmetric nature of the dithiolate. In chloroform solution, **2** exhibits two singlets at δ 5.44 and 5.38 ppm (4 H) with Pt satellites ($J_{Pt-H} = 28$ Hz) assignable to two sets of inequivalent COD vinylic protons and two sets of multiplets at δ 2.70 and 2.35 ppm, integrating to four hydrogens each, which correspond to the endo and exo protons of the COD ligand, respectively. In addition, there are two proton resonances due to the ethyl group on the dithiolate, a quartet at δ 4.25 ppm (2 H, $J_{H-H} = 17$ Hz) and a triplet at δ 1.35 ppm (3 H, $J_{H-H} = 10$ Hz).

The complexes Pt(COD)(mnt) (**1**) and Pt(COD)(ecda) (**2**) were characterized electrochemically and found by cyclic voltammetry to exhibit a single irreversible reduction ($E_{pa} = -1.74$ and -1.76 eV, respectively) in the range of -1.85 to 1.75 V vs ferrocene. There was no observable oxidation peak over the same potential range. The parent complex Pt(COD)Cl2 shows similar electrochemical behavior with an irreversible reduction ($E_{pa} = -1.64$ eV) and no oxidation over the same potential range.

The square planar geometry about the platinum in both complexes is confirmed by the single-crystal X-ray diffraction studies. The ORTEP diagrams of both complexes, Pt(COD)(mnt) (**1**) and Pt(COD)(ecda) (**2**), are shown as Figures 1 and 2, respectively. Selected bond distances and angles for both structures are presented in Table II. Also listed in Table II are the Pt–C* bond lengths where C* is defined as the midpoint of the COD double bonds that are coordinated to the Pt(II) ion. Supplementary material contains the final anisotropic thermal parameters, the calculated hydrogen positional parameters, and a complete tabulation of bond distances and angles.

The five-membered chelate ring formed in Pt(COD)(mnt) (**1**) between the Pt and mnt ligand shows some delocalization around the ring. The average Pt–S and S–C bond lengths (2.265(7) and 1.732(6) Å, respectively) are shorter than typical single bonds compared with the related platinum–thiolate complexes *trans*-Pt(SC_6F_5)$_2$L$_2$, where L = SEt_2 (Pt–S = 2.3231 Å and S–C = 1.760(7) Å of the SC_6F_5 moiety),[9] and *cis*-(*E*)-[Pt(SPh)(PhSCSO)(PPh$_3$)$_2$] (Pt–S = 2.379(4) Å and S–C = 1.791(4) Å of

---

[9] Cruz-Garritz, D.; Martin, E.; Torrens, H.; Mayoh, K. A.; Smith, A. J. *Acta Crystallogr.* **1990**, *C46*, 2377.

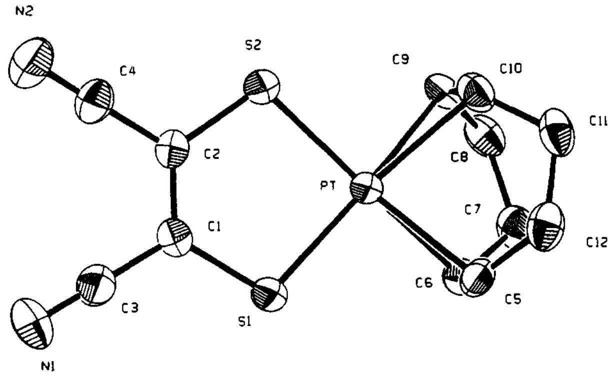

Figure 1. Molecular structure and atom numbering (ORTEP diagram, 50% thermal ellipsoids) of Pt(COD)(mnt) (**1**).

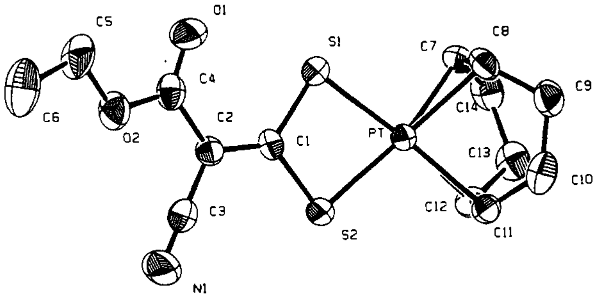

Figure 2. Molecular structure and atom numbering (ORTEP diagram, 50% thermal ellipsoids) of Pt(COD)(ecda) (**2**).

Table II. Selected Bond Distances (Å) and Angles (deg) for Pt(COD)(mnt) (**1**) and Pt(COD)(ecda) (**2**) with Atom Labels According to Figures 1 and 2, Respectively, with Estimated Standard Deviation in Parentheses

Pt(COD)(mnt) (1)		Pt(COD)(ecda) (2)	
	Distances		
Pt–S1	2.272(2)	Pt–S1	2.299(2)
Pt–S2	2.259(2)	Pt–S2	2.298(2)
Pt–C5	2.192(6)	Pt–C7	2.178(9)
Pt–C6	2.216(6)	Pt–C8	2.197(9)
Pt–C9	2.209(6)	Pt–C11	2.206(9)
Pt–C10	2.211(6)	Pt–C12	2.215(9)
S1–C1	1.732(6)	S1–C1	1.737(9)
S2–C2	1.732(6)	S2–C2	1.737(8)
C1–C2	1.368(8)	C1–C2	1.38(1)
Pt–C*1[a]	2.096(10)	Pt–C*3[c]	2.079(10)
Pt–C*2[b]	2.097(10)	Pt–C*4[d]	2.100(10)
	Angles		
S1–Pt–S2	89.78(6)	S1–Pt–S2	75.60(8)
Pt–S1–C1	103.3(2)	Pt–S1–C1	87.9(3)
Pt–S2–C2	103.2(2)	Pt–S2–C1	88.0(3)
Pt–C5–C6	72.9(4)	Pt–C7–C8	72.5(6)
Pt–C6–C5	71.0(4)	Pt–C8–C7	71.0(5)
Pt–C9–C10	71.6(4)	Pt–C11–C12	72.1(5)
Pt–C10–C9	71.5(3)	Pt–C12–C11	71.4(5)

[a] C*1 is the center of mass of C5 and C6 of **1**. [b] C*2 is the center of mass of C9 and C10 of **1**. [c] C*3 is the center of mass of C7 and C8 of **2**. [d] C*4 is the center of mass of C11 and C12 of **2**.

the SPh moiety).[10,11] The S–C bond lengths are in the range observed for other delocalized metal–dithiolate complexes (1.70–1.75 Å), where M = Ni(II), Pt(II), Co(II), and Cu(I), indicating that the bond length is independent of metal and metal oxidation state.[12-17] Also, the C1—C2 bond length of the mnt ligand is 1.368(8) Å, typical of a C=C double bond. The cyclooctadiene moiety has two localized C=C double bonds (1.38 Å) and six C—C single bonds (1.51 Å).

Table III. Room-Temperature Electronic Absorption Spectral Data in Acetonitrile and Chloroform Solutions

compd	solvent	λ, nm	ν, 10^3 cm^{-1}	ϵ_{max}, M^{-1} cm^{-1}
Pt(COD)(mnt) (**1**)	CH_3CN	275	36.4	11620
		330	30.3	7014
		346	28.9	6208
		387	25.8	590
	$CHCl_3$	268	37.3	14680
		336	29.6	9604
		348	28.7	10010
		398	25.3	668
Pt(COD)(ecda) (**2**)	CH_3CN	280	35.7	12010
		328 sh	30.5	20840
		340 sh	29.4	24590
		350	28.6	25270
		384 sh	26.0	1190
	$CHCl_3$	283	35.3	12710
		330 sh	30.3	19490
		342 sh	29.2	22360
		350	28.6	22460
		394 sh	25.4	812

For Pt(COD)(ecda) (**2**), the average Pt–S distance of 2.298(7) Å is consistent with previous reports on Pt complexes with 1,1-dithiolates such as $Pt(\textit{i}\text{-mnt})_2^{2-}$ (average Pt–S = 2.315 Å)[18] and *cis*-$Pt(PPh_3)_2(S_2C{=}CH(O)C_6H_5)$ ($Pt{-}S_1$ = 2.3202 Å and $Pt{-}S_2$ = 2.3402 Å),[19] but shorter than the corresponding single Pt—SPh bond (2.379(4) Å) in the related complex *cis*-(*E*)-$[Pt(SPh)(PhSCSO)(PPh_3)_2]$. The S–C distances (1.737(8) Å) are shorter than that expected for a typical single bond, and together with the values of the C–C bonds in the dithiolate ligand (1.381, 1.421, and 1.471 Å, respectively, for C1–C2, C2–C3, and C2–C4) suggest delocalization over the π-electron system of the ecda ligand.

As shown in Table II, Pt(COD)(mnt) (**1**) and Pt(COD)(ecda) (**2**) have similar geometries, the major difference being the S–Pt–S bite angle, which is constrained to be substantially less than 90° in the ecda complex. A possible manifestation of the geometric constraint of the ecda ligand is the slightly longer Pt–S bonds in **2** compared to **1**. All other related bond lengths, including the Pt—C* distances where C* is the midpoint of the coordinated C=C bonds of the two complexes are within experimental error.

Electronic Absorption and Emission Spectroscopy. Table III presents room-temperature electronic spectral data in acetonitrile and chloroform solutions. In contrast with the analogous spectra of the Pt(diimine)(dithiolate) complexes, the spectra of **1** and **2** exhibit no solvent sensitive absorption bands. The room-temperature absorption spectra of Pt(COD)(mnt) (**1**) and Pt(COD)(ecda) (**2**) in acetonitrile solution are shown in Figure 3. Both complexes have intense absorption bands between 325 and 375 nm. In addition, Pt(COD)(mnt) (**1**) has a well-resolved low energy band (λ_{max} = 387 nm, 25.8 kcm^{-1}), while Pt(COD)(ecda) (**2**) exhibits only a weak tail into the visible region of the spectrum.

The assignment of the absorption bands is complicated due to the number of possible transitions in these complexes including d–d, $d{-}\pi^*_{dithiolate}$, $d{-}\pi^*_{COD}$, $\pi{-}\pi^*_{dithiolate}$, and $\pi{-}\pi^*_{COD}$. Both free COD and $Pt(COD)Cl_2$ show electronic transitions having $\lambda <$ 300 nm, and neither exhibits absorptions in the 300–600-nm region of the spectrum. Since the dithiolate ligands are stronger field ligands than chloride, the $d{-}\pi^*_{COD}$ transition in Pt(COD)(S-S) should occur at higher energy relative to that in $Pt(COD)Cl_2$.

---

(10) Gosselink, J. W.; Brouwers, A. M. F.; von Koten, G.; Vrieze, K. *J. Chem. Soc., Chem. Commun.* **1979**, 1045.
(11) Gosselink, J. W.; von Koten, G.; Brouwers, A. M. F.; Overbeek, O. *J. Chem. Soc., Dalton Trans.* **1981**, 342.
(12) Günter, W.; Gliemann, G.; Klement, U.; Zabel, M. *Inorg. Chim. Acta* **1989**, *165*, 51.
(13) Welch, J. H.; Bereman, R.; Singh, P. *Inorg. Chim. Acta* **1989**, *163*, 93.
(14) Kobayashi, A.; Sasaki, Y. *Bull. Chem. Soc. Jpn.* **1977**, *50*, 2650.
(15) Coucouvanis, D.; Baenziger, N. C.; Johnson, S. M. *Inorg. Chem.* **1974**, *13*, 1191.
(16) Eisenberg, R.; Ibers, J. A. *Inorg. Chem.* **1965**, *4*, 605.
(17) Forrester, J. D.; Zalkin, A.; Templeton, D. H. *Inorg. Chem.* **1964**, *3*, 1507.
(18) Hummel, H-U. *Transition Met. Chem.* (*Weinheim, Ger.*) **1987**, *12*, 172.
(19) Weigand, W.; Bosl, G.; Polborn, K. *Chem. Ber.* **1990**, *123*, 1339.

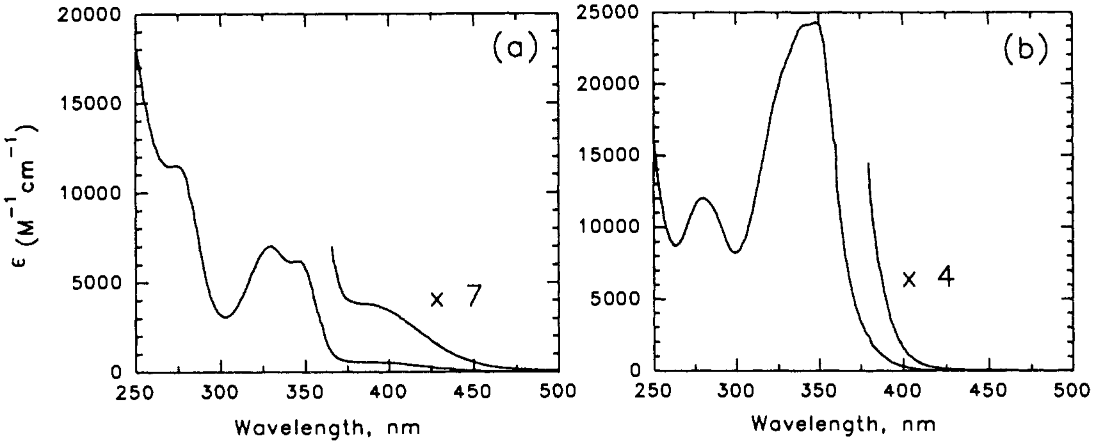

Figure 3. Room temperature electronic absorption spectrum in acetonitrile solution of (a) Pt(COD)(mnt) (**1**) and (b) Pt(COD)(ecda) (**2**).

The only absorption band with $\lambda < 300$ nm in complexes **1** and **2** occurs at 275 nm (36.4 kcm^{-1}) and 280 nm (35.7 kcm^{-1}), respectively. This band may be attributed to a d–π^*_{COD} transition, although a π–π^*_{COD} transition cannot be ruled out.

There are at least two intense absorption bands between 325 and 375 nm in both complexes as shown in Figure 3. We believe that these transitions involve the dithiolate moiety because they are absent in free COD and in Pt(COD)Cl_2 while intense visible absorptions are present in the following related compounds: Na_2(mnt), K_2(ecda), $TBA_2[Pt(mnt)_2]$, and $TBA_2[Pt(ecda)_2]$. Detailed assignments of the absorption spectra of $Pt(mnt)_2^{2-}$ and $Pt(i\text{-mnt})_2^{2-}$ have appeared in the literature.[20-22] The electronic absorption spectrum of $Pt(mnt)_2^{2-}$ contains six bands between 300 and 700 nm. The highest energy absorptions at 309 and 336 nm (ϵ_{max} = 13 400 and 15 600 M^{-1} cm^{-1}, respectively) are due to π–$\pi^*_{\text{dithiolate}}$ transitions, while bands at 473 and 540 nm (ϵ_{max} = 3470 and 1220 M^{-1} cm^{-1}, respectively) are assigned as metal-to-dithiolate charge transfer transitions. Also, two low energy transitions at 639 and 694 nm (ϵ_{max} = 56 and 49 M^{-1} cm^{-1}, respectively) originate from metal d–d absorptions. The electronic absorption spectrum of $Pt(i\text{-mnt})_2^{2-}$ is similar to that of $Pt(mnt)_2^{2-}$ except that no low energy d–d transitions are reported in the same spectral region. Two absorptions at 312 and 352 nm (ϵ_{max} = 18 000 and 3500 M^{-1} cm^{-1}, respectively) originate from π–$\pi^*_{\text{dithiolate}}$ transitions, and the MLCT transition occurs at 413 nm (ϵ_{max} = 55 000 M^{-1} cm^{-1}). For Pt(COD)(mnt) (**1**), the bands at ~330 and 346 nm most likely arise from d–$\pi^*_{\text{dithiolate}}$ transitions. The analogous transitions for Pt(COD)(ecda) (**2**) occur at 340 and 350 nm and dominate the electronic spectrum. The shifts to higher energy for the d–$\pi^*_{\text{dithiolate}}$ transition in the Pt(COD)(dithiolate) complexes relative to the $Pt(S\text{-}S)_2^{2-}$ complexes is expected since in the neutral species the d orbitals are more contracted and lie at lower energies than in the dianionic complexes.

The lowest energy transition in **1** and the low energy shoulder in **2** that yields low temperature emission upon irradiation are most likely due to a spin forbidden process such as a d–d or the triplet d–$\pi^*_{\text{dithiolate}}$ transition based on its low molar extinction coefficient. These assignments will be discussed further after consideration of the emission spectroscopy.

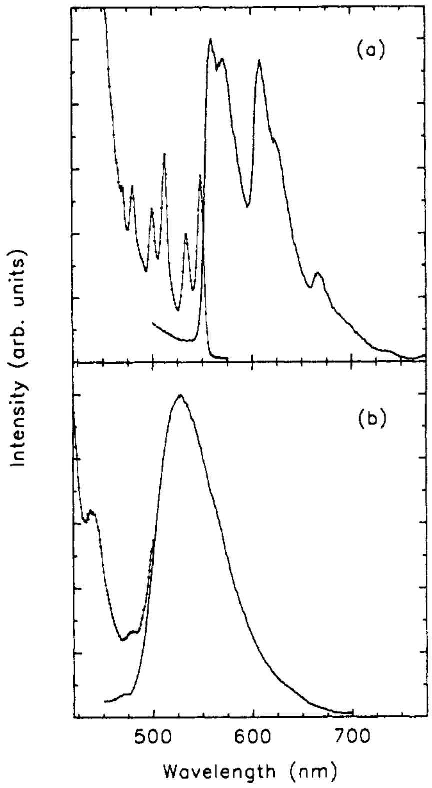

Figure 4. Low temperature emission (—, solid state, 77 K) and excitation (- - -, solid state, 77 K) spectra of (a) Pt(COD)(mnt) (**1**) and (b) Pt(COD)(ecda) (**2**).

Table IV. Electronic Emission and Excitation Spectral Data at 77 K in Solid KBr Matrix and in Rigid DMM[a] Glass

compd	matrix	highest energy em max, nm[b]	lowest energy exc max, nm[b]	lifetime, μs
Pt(COD)(mnt)	KBr	560 (17.9)	549 (18.2)	
(1)	DMM	583 (17.2)	547 (18.3)	74.2
Pt(COD)(ecda)	KBr	525 (19.0)	441 (22.7)	
(2)	DMM	541 (18.5)	455 (22.0)	17.5, 148

[a] DMF/methylene chloride/methanol (1:1:1 v/v/v). [b] Values in parentheses are reported in wavenumbers, $\times 10^3$ cm^{-1}.

The Pt(COD)(mnt) (**1**) complex luminesces weakly at room temperature in the solid state, while Pt(COD)(ecda) (**2**) in the solid state shows emission only at low temperature. Neither complex luminesces in fluid solution but both are found to emit in rigid DMM glasses (DMF/methylene chloride/methanol in 1:1:1 v/v/v) at 77 K. The emission spectra from the DMM glasses were less resolved than the solid-state emissions. Figure 4 presents the low temperature emission and excitation spectra in KBr matrix for both complexes, while Table IV gives the highest energy emission and lowest energy excitation maxima at 77 K, along with emission lifetime data.

The 77 K solid-state emission spectra of the two complexes differ greatly and are characteristic of the respective dithiolate

---

[20] Shupack, S. I.; Billig, E.; Clark, R. J. H.; Williams, R.; Gray, H. B. *J. Am. Chem. Soc.* **1964**, *86*, 4594.

[21] Werden, B. G.; Billig, E.; Gray, H. B. *Inorg. Chem.* **1966**, *5*, 10027.

[22] The ligand *i*-mnt has –CN in place of the –COOEt functionality of ecda. As outlined in ref 2, the optical properties of analogous complexes prepared with ecda and with *i*-mnt are virtually identical.

ligands. As shown in Figure 4, the emission spectrum of Pt(COD)(mnt) (**1**) exhibits a large vibrational progression of ~1440 cm^{-1} which has been attributed previously to the localized C=C stretch (1427 cm^{-1}) of the mnt ligand[5] in Pt(COD)(mnt) as well as a smaller progression of ~470 cm^{-1}. For Pt(COD)(ecda) (**2**) the emission is broad (fwhm = 2550 cm^{-1}), featureless, and blue-shifted with respect to the mnt complex. The excitation spectra also show similar differences. The excitation spectrum of Pt(COD)(mnt) (**1**) exhibits sharp, well-defined bands with a large progression of ~1300 cm^{-1} and a smaller spacing of ~500 cm^{-1}, whereas for Pt(COD)(ecda) (**2**), the spectrum is fairly featureless and is again blue shifted with respect to **1**.

Previous results from our laboratory reveal that the shape and energy of the emission band from different PtL_2(S-S) complexes where L_2 is either chelating phosphine or bis(phosphine) ligands show a similar dependence on the dithiolate ligand as that seen for **1** and **2**.[23] All PtL_2(mnt) complexes possess highly structured emission profiles whereas the emission bands from PtL_2(ecda) complexes are broad and asymmetric. The nature of the 77 K emission spectrum in either the solid state or frozen glass thus appears to be independent of L. The emission spectra from two related (±)-*trans*-diaminocyclohexane (tdach) complexes, Pt(tdach)(mnt) and Pt(tdach)(ecda), were recently reported[24] and they also show the same characteristics—*i.e.*, a structured emission band from Pt(tdach)(mnt) (λ_{max} = 610 nm, 16.4 kcm^{-1}) and a broad and asymmetric emission from Pt(tdach)(ecda) (λ_{max} = 540 nm, 18.5 kcm^{-1}). All of these results strongly support the view that the emissive state in these Pt(II) complexes involves the dithiolate ligand.

The nature of the excited state in square planar dithiolate complexes has been explored previously by us.[5] Complexes of the type $MLL'(mnt)^{n-}$ (n = 1, M = Ir, Rh; n = 0, M = Pt; L, L′ = PR_3, $P(OR)_3$, CO, dppe) were also shown to have highly structured emission spectra at 77 K. On the basis of the similarity of the emission profile from all of the mnt complexes as well as a shift in λ_{em} with electron donating ability of L and L′, an emissive state of metal-to-π^*_{mnt} charge transfer was assigned. In addition, extended Hückel molecular orbital calculations performed on the platinum(II) diimine dithiolate complexes[24] are consistent with the MLCT assignment of complexes **1** and **2**. Specifically, the semiempirical calculations show that the lowest unoccupied $\pi^*_{dithiolate}$ levels lie below the metal $d\sigma^*$ orbital of these square planar complexes and that the π^*_{mnt} level lies lower in energy than the $\pi^*_{i\text{-}mnt}$ orbital for a given Pt(diimine) moiety (*i*-mnt differs from ecda in having the –COOEt functionality replaced by –CN and was used for computational simplicity).[24] This is consistent with the relative energy of λ_{em} for the two complexes, being 583 nm for **1** and 541 nm for **2** in DMM glass and suggest that mnt is a better π-acid than *i*-mnt (or ecda). For complexes **1** and **2** relative to the Pt(II) diimine dithiolate systems studied previously,[1–4,24] the absence of a $\pi^*_{diimine}$ level results in the absence of a solvatochromic charge transfer band of partial *inter*ligand character and makes the assignment of the lowest energy emissive state relatively straightforward as $d\text{–}\pi^*_{dithiolate}$. The difference in the appearance of the emission from **1** and **2**, and from mnt and ecda complexes in general, relates to differences in the $\pi^*_{dithiolate}$ orbital and electronic structure of the two ligands. The mnt ligand upon complexation forms a 5-membered chelate ring that contains a C=C double bond while ecda forms a 4-membered chelate ring with an exo C=C double bond; the $\pi^*_{dithiolate}$ orbitals are consequently different.

Lifetime measurements for **1** and **2** were done in rigid DMM glass at 77 K by transient digitization. Emission lifetimes are in the 10–100-μs range and are given in Table IV. Complex **1** shows a single exponential decay lifetime whereas complex **2** exhibits double exponential decay which may indicate the presence of multiple state emission. Analogous ecda complexes in which COD is replace by phosphine ligands show similar double exponential decay behavior.[23] Multiple state emission is not uncommon and has been observed in many platinum complexes including those studied by Gliemann *et al.*[25] and Barigelletti and Balzani *et al.*[26] Further study is required to get information on the kinetics of the states involved with this emission.

The relatively long lifetimes of these complexes indicate that there is substantial spin-forbidden character in their emissive excited state, although spin selection rules may be relaxed considerably due to the large spin–orbit coupling of platinum.[27] On the basis of these results and previous studies that show the emission to be dependent on the nature of the dithiolate, the emissive state for both COD dithiolate complexes **1** and **2** is assigned as a $^3\{d\text{–}\pi^*_{dithiolate}\}$ state.

Conclusions

The complexes Pt(COD)(mnt) and Pt(COD)(ecda) were synthesized to examine their emission behavior and probe the effect of the dithiolate on their luminescence. The structures of both complexes were established by single-crystal X-ray structure determinations and the spectroscopic properties of both complexes were compared. Complexes **1** and **2** possess square-planar coordination geometries with metrical parameters of the dithiolate chelate rings giving evidence of delocalization. Both complexes are emissive in the solid state and in rigid media at low temperature but the shape of their emission bands are very different. On the basis of the emission results including lifetimes, on comparison with other emissive dithiolate complexes and on molecular orbital calculations for d^8 diimine dithiolate systems, the emissive state for each complex is assigned as $^3\{d\text{–}\pi^*_{dithiolate}\}$. The difference in the emission profile for the two complexes—highly structured for Pt(COD)(mnt) (**1**) with a major progression of 1440 cm^{-1} and broad and featureless for Pt(COD)(ecda) (**2**)—relate to the difference between the lowest π^* orbital for the two ligand systems studied here, mnt and ecda.

Acknowledgment. We wish to thank the U.S. Department of Energy, Division of Chemical Sciences for support of this research and Johnson Matthey Aesar/Alfa Co. for a generous loan of platinum salts.

Supplementary Material Available: Complete listing of crystallographic details, bond lengths and bond angles, positional and isotropic thermal parameters, and anisotropic thermal parameters for **1** and **2** (11 pages). Ordering information is given on any current masthead page.

---

(23) Bevilacqua, J. M.; Zuleta, J. A.; Eisenberg, R. Paper in preparation.

(24) Zuleta, J. A.; Bevilacqua, J. M.; Proserpio, D. M.; Harvey, P. D.; Eisenberg, R. *Inorg. Chem.* **1992**, *31*, 2396.

(25) For example, Biedermann, J.; Gliemann, G.; Klement, U.; Range, K.-J.; Zabel, M. *Inorg. Chim. Acta* **1990**, *171*, 35; Schlattl, K.; Gliemann, G.; Jolliet, P.; von Zelewsky, A. *Chem. Phys. Lett.* **1990**, *168*, 505.

(26) For example, Barigelletti, F.; Sandrini, D.; Maestri, M.; Balzani, V.; von Zelewsky, A.; Chassot, L.; Jolliet, P.; Maeder, U. *Inorg. Chem.* **1988**, *27*, 3644 and references cited therein.

(27) Crosby, G. A.; Hipps, K. W.; Elfring, W. H. *J. Am. Chem. Soc.* **1974**, *96*, 629.